

# On the Rate of Error Growth in Time for Numerical Solutions of Nonlinear Dispersive Wave Equations

Hendrik Ranocha<sup>\*1</sup>, Manuel Quezada de Luna<sup>†1</sup>, and David I. Ketcheson<sup>‡1</sup>

<sup>1</sup>King Abdullah University of Science and Technology (KAUST), Computer Electrical and Mathematical Science and Engineering Division (CEMSE), Thuwal, 23955-6900, Saudi Arabia

February 15, 2021

We study the numerical error in solitary wave solutions of nonlinear dispersive wave equations. A number of existing results for discretizations of solitary wave solutions of particular equations indicate that the error grows quadratically in time for numerical methods that do not conserve energy, but grows only linearly for conservative methods. We provide numerical experiments suggesting that this result extends to a very broad class of equations and numerical methods.

**Key words.** invariant conservation, summation by parts, spectral collocation methods, relaxation schemes, error growth rate

**AMS subject classification.** 65M12, 65M70, 65M06, 65M60, 65M20, 35Q35

## 1 Introduction

All numerical schemes for solving partial differential equations (PDEs) commit truncation errors. In order to provide accurate answers, it is essential that these errors be small (the scheme must be consistent) and propagate without blowing up (the scheme must be stable). Some numerical schemes have the additional capability to completely eliminate

---

\*ORCID: 0000-0002-3456-2277

†ORCID: 0000-0001-7288-0367

‡ORCID: 0000-0002-1212-126X

certain kinds of errors – to ensure the numerical solution lie on some lower-dimensional manifold. This is typically done in order to mimic a corresponding property of the solution itself (such as conservation of energy). The general philosophical motivation for this approach is to ensure that the approximate solution not only is close to the true solution for the given initial data, but that it lies within the set of possible exact solutions for some initial data. This concept is similar to backward stability: an approximate solution that lies on the desired manifold is possibly the exact solution to a problem with different initial data, whereas a solution that lies off the manifold cannot be the exact solution to the PDE for any initial data.

Methods that impose such a qualitative constraint can also lead to a quantitative reduction in the overall error. This has been shown to be the case for several numerical approximations of Hamiltonian systems. In particular, whereas numerical solutions generically exhibit quadratic error growth in time, solutions that exactly conserve a nonlinear invariant yield only linear error growth. This has been shown for finite-dimensional systems [9, 11, 12, 20], and for solitary wave solutions of the Korteweg-de Vries equation [15], the nonlinear Schrödinger equation [21], Peregrine’s regularized long wave (RLW) equation (also known as the Benjamin-Bona-Mahoney (BBM) equation [5, 42]), and the generalized BBM equation [19]. The results in [19, 42] are purely experimental, while the remaining results just cited include proofs along with numerical demonstrations.

The PDE results in this direction are all specific to solitary wave solutions. The conservative discretizations that yield linear error growth also exhibit *modified solitary waves* [5, 19]. These are discrete solitary waves that are close to but different from the exact solitary wave solutions. The ability of these modified solitary waves to propagate discretely without changing shape or amplitude means that conservative methods are appealing for long-time simulations of solitary waves and their interactions [18]. The concept of a modified solitary wave also provides an intuitive rough explanation of the observed error growth rates. In a non-conservative method, the solitary wave is approximated by a wave whose amplitude grows or diminishes linearly in time. Since the speed of the solitary wave is (at least to first approximation) a linear function of the amplitude, the error in the speed of the wave also grows linearly in time. This leads to a quadratic error in the location (phase) of the wave. Meanwhile, it was shown in [5, 19] that a conservative scheme yields a modified solitary wave whose amplitude and speed are constant in time (though different from those of the true solitary wave). Hence the error in the position grows only linearly.

While the examples that have been given are suggestive, the results on linear error growth in the literature are in some cases only experimental and in others rely on particular properties of the system in question. The pattern of these results suggests the possibility of a much broader phenomenon; an important question then is how general this behavior is, in terms of differential equation systems, conserved quantities, and numerical methods. In this work we provide strong evidence that it extends to a very large class of dispersive wave equations and nonlinear invariants, including invariants that are not quadratic, and even certain solutions of first-order hyperbolic systems that have no dispersive terms.

We briefly introduce the spatial and temporal discretization methods we will use in Section 2. In Section 3, we analyze the temporal error growth of solitary wave solutions to several nonlinear dispersive wave equations. Our experimental results include the Fornberg-Whitham [69], Camassa-Holm [10], Degasperis-Procesi [16], Holm-Hone [30], and BBM-BBM equations [7, 8]. For each of these models, we apply recently-constructed conservative schemes and show experimentally that they yield improved (linear) error growth when compared to non-conservative schemes for the same model. To demonstrate

the importance of nonlinearity for the different error growth behaviors of conservative and non-conservative methods, we investigate a linear dispersive wave equation in Section 4. There, both kinds of methods result in the same asymptotic error growth rate, although the absolute error of the conservative method is smaller. We then go further outside the realm of available results and consider two first-order nonlinear hyperbolic systems that have been shown to possess solitary-wave-like solutions. In Section 5 we study the variable-coefficient  $p$ -system in one dimension, with periodically varying coefficients. Previous work on this system has noted similarities with dispersive nonlinear wave equations; see [33, 38]. In Section 6, we study the two-dimensional shallow water equations with varying bathymetry. Finally, we summarize and discuss our results in Section 7.

The source code used to generate the results of this study is available online [57]. The numerical methods studied in this article are implemented in Julia [6]. We use time integration methods from [49]. The plots are generated using Matplotlib [31].

## 2 Introduction of the discretization methods

In this section, we will briefly introduce the type of discretization methods employed in this article.

### 2.1 Spatial semidiscretizations

Proving the conservation of invariants of partial differential equations usually requires the product/chain rule and integration by parts. It is often useful to mimic the same procedure at the discrete level by using summation by parts (SBP) operators, which are constructed specifically to satisfy a discrete analogue of integration by parts. A review of the relevant theory can be found in [13, 22, 66]. Many classes of numerical methods can be formulated within the SBP framework, including finite difference [65], finite volume [44, 45], continuous Galerkin [1, 28, 29], discontinuous Galerkin [25], and flux reconstruction methods [59]. A brief review of how to formulate these methods in the SBP framework with application to structure-preserving numerical methods used in this article is given in [58].

Next, we will briefly introduce SBP operators in periodic domains in one space dimension. Extensions to multiple space dimensions can be achieved via tensor products. We consider a grid  $\mathbf{x} = (x_1, \dots, x_m)$  where  $x_1 = x_{\min} \leq x_2 \cdots \leq x_m = x_{\max}$ . All nonlinear operations will be performed pointwise, i.e. we use a collocation approach.

**Definition 2.1.** Given a grid  $\mathbf{x}$ , a  $p$ -th order accurate  $i$ -th derivative matrix  $D_i$  is a matrix that satisfies

$$\forall k \in \{0, \dots, p\}: \quad D_i \mathbf{x}^k = k(k-1) \dots (k-i+1) \mathbf{x}^{k-i}, \quad (2.1)$$

with the convention  $\mathbf{x}^0 = \mathbf{1}$  and  $0\mathbf{x}^k = \mathbf{0}$ . We say  $D_i$  is consistent if  $p \geq 0$ .  $\triangleleft$

For periodic boundary conditions (under which  $x_{\min}$  and  $x_{\max}$  are identical), integration by parts is basically a statement about the symmetry of a derivative operator with respect to the  $L^2$  scalar product. Discretely, an approximation of this scalar product is represented by a so-called mass matrix  $M$ .<sup>1</sup>

---

<sup>1</sup>The name *mass matrix* is common in the finite element literature. In classical articles on finite difference SBP operators, this matrix is often called a *norm matrix*.

**Definition 2.2.** A *periodic first-derivative SBP operator* consists of a grid  $\mathbf{x}$ , a consistent first-derivative matrix  $D_1$ , and a symmetric and positive-definite matrix  $M$  such that

$$MD_1 + D_1^T M = 0. \quad (2.2)$$

◀

We will often refer to an operator  $D_i$  as a (periodic) SBP operator if the other operators (such as the mass matrix  $M$ ) are clear from the context. We always assume derivative operators are consistent, but we will usually omit this term.

**Definition 2.3.** A *periodic second-derivative SBP operator* consists of a grid  $\mathbf{x}$ , a consistent second-derivative matrix  $D_2$ , and a symmetric and positive-definite matrix  $M$  such that

$$MD_2 = -A_2, \quad A_2 \text{ is symmetric and positive semidefinite.} \quad (2.3)$$

◀

**Definition 2.4.** A *periodic fourth-derivative SBP operator* consists of a grid  $\mathbf{x}$ , a consistent fourth-derivative matrix  $D_4$ , and a symmetric and positive-definite matrix  $M$  such that

$$MD_4 = A_4, \quad A_4 \text{ is symmetric and positive semidefinite.} \quad (2.4)$$

◀

In the following, we will use Fourier (pseudospectral) collocation methods [24, 37] because of their efficiency and accuracy for smooth problems. Nevertheless, all classes of methods within the SBP framework can be used and analyzed interchangeably to construct conservative semidiscretizations.

## 2.2 Time integration methods

To transfer the semidiscrete conservation results to fully-discrete schemes, the recent relaxation approach is used [32, 54–56, 60]. Related ideas date back to [62, 63] and [17, pp. 265–266] but have been developed widely just recently.

Semidiscretizations reduce an initial boundary value PDE to an initial value ODE

$$u'(t) = f(u(t)), \quad u(0) = u^0. \quad (2.5)$$

Throughout this work we use superscripts to denote the time step, and here  $u^0$  is the initial condition. To conserve a nonlinear invariant functional  $J(u)$  discretely in a one-step method, we require  $J(u^n) = J(u^{n-1}) = J(u^0)$ . For a Runge-Kutta method

$$y_i = u^n + \Delta t \sum_{j=1}^s a_{ij} f(t_n + c_j \Delta t, y_j), \quad i \in \{1, \dots, s\}, \quad (2.6a)$$

$$u(t_n + \Delta t) \approx u^{n+1} = u^n + \Delta t \sum_{i=1}^s b_i f(t_n + c_i \Delta t, y_i), \quad (2.6b)$$

we define the update direction

$$d^n := \sum_{i=1}^s b_i f_i, \quad (2.7)$$

where we use the abbreviation  $f_i := f(t_n + c_i \Delta t, y_i)$ . Since the new solution  $u^n$  will not be conservative in general, we modify the update formula (2.6b) by introducing a relaxation parameter  $\gamma^n$  and use

$$u(t_n + \gamma^n \Delta t) \approx u_\gamma^{n+1} = u^n + \gamma^n \Delta t d^n. \quad (2.8)$$

To guarantee conservation of  $J$ ,  $\gamma^n$  is computed as root of

$$J(u_\gamma^{n+1}) = J(u^n). \quad (2.9)$$

This scalar nonlinear equation can be solved efficiently using algorithms such as the one of [2]. By the general theory on relaxation methods, there is exactly one root  $\gamma^n = 1 + O(\Delta t^{p-1})$  of (2.9) [56, Theorem 2.14]. By construction of the relaxation parameter  $\gamma^n$ , the resulting solution  $u_\gamma^{n+1}$  conserves the invariant  $J$ . Moreover, the relaxation approach also automatically conserves linear invariants (as long as the semi-discretization conserves them), which is an important prerequisite of analytical results on linear vs. quadratic error growth in time. Finally, the solution (2.8) has the same local order of accuracy as that given by the original Runge-Kutta method (2.6).

### 3 Nonlinear dispersive wave equations

In this section we consider several nonlinear dispersive wave equations. Conservative numerical methods for these equations have been developed and analyzed in [58] using various classes of SBP operators. We will use split forms to preserve local conservation laws, since the chain and product rules cannot hold discretely for many high-order discretizations [52]. These are related to entropy-conservative methods in the sense of Tadmor [67]. While certain split forms have been known for some time [61, eq. (6.40)], they are still state of the art and enable the construction of numerical methods with desirable properties [27, 51, 64, 71].

For each equation, after reviewing the split-form conservative spatial discretization, we present a numerical test of error growth for a solitary wave solution. The solitary wave solutions are obtained via the Petviashvili method [48] using a Fourier collocation method with  $2^{16}$  nodes. The resulting solitary wave profile is interpolated to a grid using fewer nodes and used as initial condition. A conservative semidiscretization is obtained by using Fourier collocation differentiation matrices in space. This semidiscretization is integrated in time using the fifth-order accurate Runge-Kutta method of Tsitouras [68] with adaptive time stepping based on local error estimates. We show results for both this method without relaxation (non-conservative) and with relaxation in time (conservative). The errors plotted are discrete  $L^2$  errors computed using the discrete norm induced by the mass matrix  $M$ , which is the identity matrix times the grid spacing for Fourier collocation methods.

### 3.1 Fornberg-Whitham equation

The Fornberg-Whitham equation [69]

$$\begin{aligned} (\mathbb{I} - \partial_x^2) \partial_t u(t, x) + (\mathbb{I} - \partial_x^2) \partial_x f(u(t, x)) + \partial_x u(t, x) &= 0, & t \in (0, T), x \in (x_{\min}, x_{\max}), \\ u(0, x) &= u^0(x), & x \in [x_{\min}, x_{\max}], \\ f(u) &= \frac{u^2}{2}, \end{aligned} \quad (3.1)$$

with periodic boundary conditions can also be written as

$$\partial_t u(t, x) + \partial_x f(u(t, x)) + (\mathbb{I} - \partial_{x,p}^2)^{-1} \partial_x u(t, x) = 0, \quad (3.2)$$

where  $(\mathbb{I} - \partial_{x,p}^2)^{-1}$  is the inverse of the elliptic operator  $\mathbb{I} - \partial_x^2$  with periodic boundary conditions. The functionals

$$J_1^{\text{FW}}(u) = \int_{x_{\min}}^{x_{\max}} u, \quad (3.3a)$$

$$J_2^{\text{FW}}(u) = \int_{x_{\min}}^{x_{\max}} (u - \partial_x^2 u), \quad (3.3b)$$

$$J_3^{\text{FW}}(u) = \int_{x_{\min}}^{x_{\max}} u^2, \quad (3.3c)$$

are invariants of solutions. All of these are conserved by semidiscretizations of the form

$$\partial_t \mathbf{u} + \frac{1}{3} D_1 \mathbf{u}^2 + \frac{1}{3} \mathbf{u} D_1 \mathbf{u} + (\mathbb{I} - D_2)^{-1} D_1 \mathbf{u} = \mathbf{0} \quad (3.4)$$

whenever  $D_1, D_2$  are commuting periodic first- and second-derivative SBP operators with diagonal mass matrix [58].

We use a numerically generated solitary wave solution as initial condition in the periodic domain  $[-80, 80]$ . We apply (3.4) with Fourier collocation differentiation matrices  $D_1, D_2$  in space and Tsitouras' fifth-order Runge-Kutta method [68] in time, with or without using relaxation to enforce conservation of (3.3c). The error growth is shown in Figure 1 for  $2^8$  nodes and a local error tolerance of  $10^{-5}$ . After an initial transient period, the error of the non-conservative scheme grows quadratically while the corresponding conservative method results in approximately linear error growth. The error of the non-conservative method starts to saturate at  $t \approx 6 \times 10^4$  since the numerical and reference waves do not overlap anymore.

### 3.2 Camassa-Holm equation

The Camassa-Holm equation [10]

$$\begin{aligned} (\mathbb{I} - \partial_x^2) \partial_t u(t, x) + \partial_x \left( \frac{3}{2} u(t, x)^2 - \frac{1}{2} (\partial_x u(t, x))^2 - u(t, x) \partial_x^2 u(t, x) \right) &= 0, \\ u(0, x) &= u^0(x), \end{aligned} \quad (3.5)$$

with periodic boundary conditions can also be written as

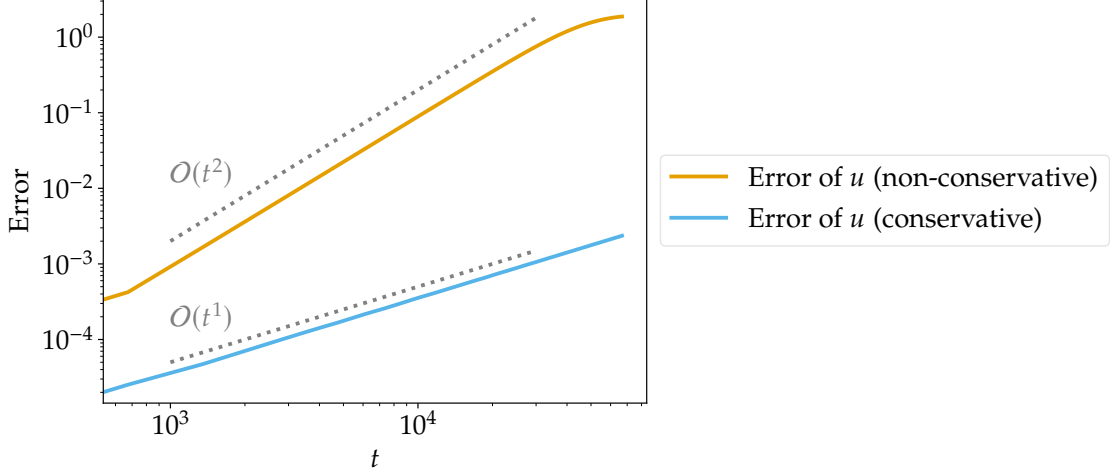


Figure 1: Error growth in time for a numerically generated solitary wave solution of the Fornberg-Whitham equation (3.1), using (3.4) with Fourier collocation in space and 5th-order Runge-Kutta in time. The conservative method uses relaxation to enforce conservation of (3.3c).

$$\partial_t u + (\mathbf{I} - \partial_{x,p}^2)^{-1} (\partial_x u^2 + u \partial_x u - \alpha \partial_x (u \partial_x^2 u) - (1 - \alpha) \partial_x^2 (u \partial_x u) - (2\alpha - 1) (\partial_x u) (\partial_x^2 u)) = 0, \quad (3.6)$$

where  $(\mathbf{I} - \partial_{x,p}^2)^{-1}$  is the inverse of the elliptic operator  $\mathbf{I} - \partial_x^2$  with periodic boundary conditions and  $\alpha \in \mathbb{R}$  is a parameter determining the split form [58]. The functionals

$$J_1^{\text{CH}}(u) = \int_{x_{\min}}^{x_{\max}} u, \quad (3.7a)$$

$$J_2^{\text{CH}}(u) = \frac{1}{2} \int_{x_{\min}}^{x_{\max}} (u^2 + (\partial_x u)^2) = \frac{1}{2} \int_{x_{\min}}^{x_{\max}} u (\mathbf{I} - \partial_x^2) u, \quad (3.7b)$$

are invariants of solutions. All of these are conserved by semidiscretizations of the form

$$\partial_t \mathbf{u} + (\mathbf{I} - D_2)^{-1} (D_1 \mathbf{u}^2 + \mathbf{u} D_1 \mathbf{u} - \frac{1}{2} D_1 (\mathbf{u} D_2 \mathbf{u}) - \frac{1}{2} D_2 (\mathbf{u} D_1 \mathbf{u})) = \mathbf{0} \quad (3.8)$$

whenever  $D_1, D_2$  are periodic first- and second-derivative SBP operators with diagonal mass matrix [58].

We use a numerically generated solitary wave solution as initial condition in the periodic domain  $[-40, 40]$ . We apply (3.8) with Fourier collocation differentiation matrices  $D_1, D_2$  in space and Tsitouras' fifth-order Runge-Kutta method [68] in time, with or without using relaxation to enforce conservation of (3.7b). The error growth is shown in Figure 2 for  $2^9$  nodes and a local error tolerance of  $10^{-7}$ . After an initial transient period, the error of the non-conservative scheme grows quadratically while the corresponding conservative method results in approximately linear error growth. The error of the non-conservative method starts to saturate at  $t \approx 10^4$  since the numerical and reference waves do not overlap anymore.

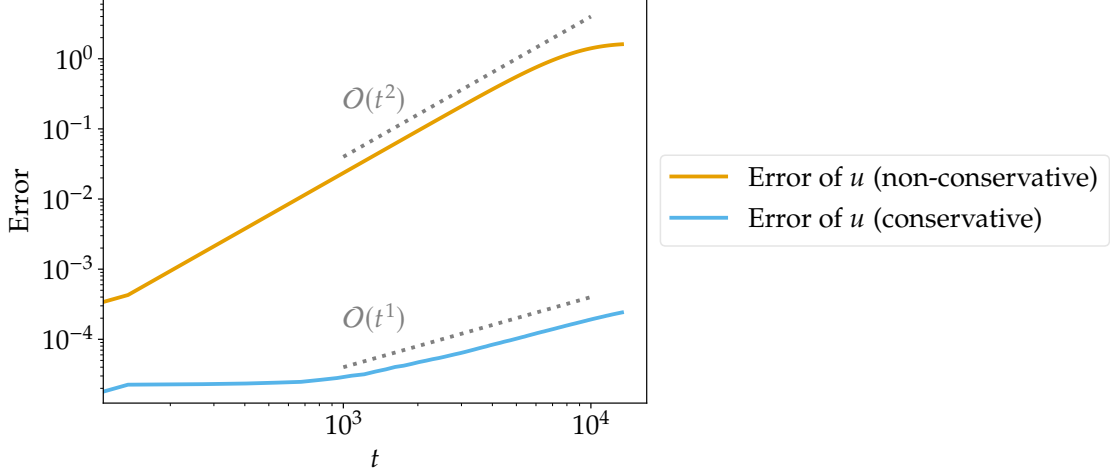


Figure 2: Error growth in time for a numerically generated solitary wave solution of the Camassa-Holm equation (3.5), using (3.8) with Fourier collocation in space and 5th-order Runge-Kutta in time. The conservative method uses relaxation to enforce conservation of (3.7b).

### 3.3 Degasperis-Procesi equation

The Degasperis-Procesi equation [16]

$$\begin{aligned}
 (\mathbf{I} - \partial_x^2) \partial_t u(t, x) + 4 \partial_x f(u(t, x)) - \partial_x^3 f(u(t, x)) &= 0, & t \in (0, T), x \in (x_{\min}, x_{\max}), \\
 u(0, x) &= u^0(x), & x \in [x_{\min}, x_{\max}], \\
 f(u) &= \frac{u^2}{2},
 \end{aligned} \tag{3.9}$$

with periodic boundary conditions can also be written as

$$\partial_t u(t, x) + (\mathbf{I} - \partial_{x,p}^2)^{-1} (4\mathbf{I} - \partial_x^2) \partial_x f(u(t, x)) = 0, \tag{3.10}$$

where  $(\mathbf{I} - \partial_{x,p}^2)^{-1}$  is the inverse of the elliptic operator  $\mathbf{I} - \partial_x^2$  with periodic boundary conditions. The functionals

$$J_1^{\text{DP}}(u) = \int_{x_{\min}}^{x_{\max}} (u - \partial_x^2 u), \tag{3.11a}$$

$$J_2^{\text{DP}}(u) = \frac{1}{2} \int_{x_{\min}}^{x_{\max}} ((u - \partial_x^2 u)v), \quad v = (4\mathbf{I} - \partial_{x,p}^2)^{-1} u, \tag{3.11b}$$

are invariants of solutions. All of these are conserved by semidiscretizations of the form

$$\partial_t \mathbf{u} + \frac{1}{3} (\mathbf{I} - D_2)^{-1} (4\mathbf{I} - D_2) (D_1 \mathbf{u}^2 + \mathbf{u} D_1 \mathbf{u}) = \mathbf{0} \tag{3.12}$$

whenever  $D_1, D_2$  are periodic first- and second-derivative SBP operators with diagonal mass matrix [58].

We use a numerically generated solitary wave solution as initial condition in the periodic domain  $[-40, 40]$ . We apply (3.12) with Fourier collocation differentiation matrices  $D_1, D_2$  in space and Tsitouras' fifth-order Runge-Kutta method [68] in time, with or without using relaxation to enforce conservation of (3.11b). The error growth is shown in Figure 3 for



$2^8$  nodes and a local error tolerance of  $10^{-5}$ . After an initial transient period, the error of the non-conservative scheme grows quadratically while the corresponding conservative method results in approximately linear error growth. The error of the non-conservative method starts to saturate at  $t \approx 10^3$  since the numerical and reference waves do not overlap anymore.

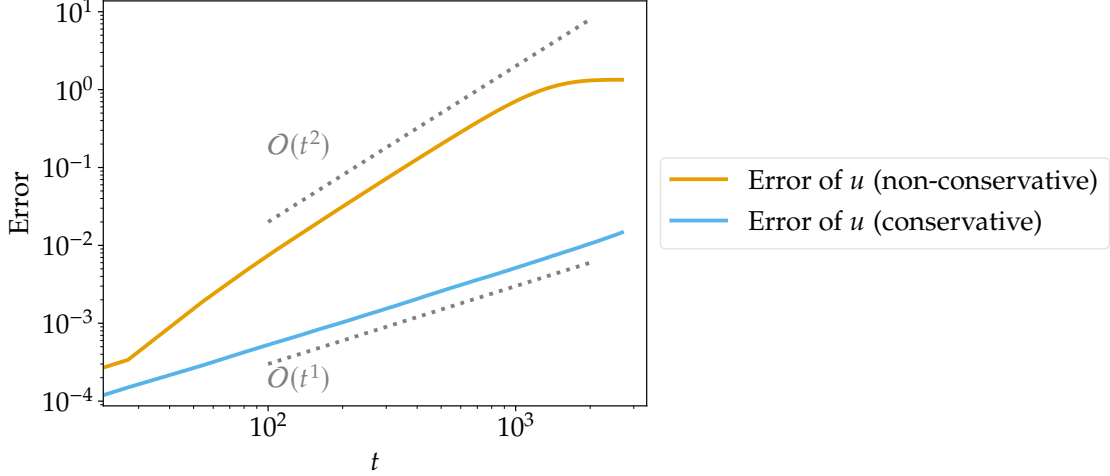


Figure 3: Error growth in time for a numerically generated solitary wave solution of the Degasperis-Procesi equation (3.9), using (3.12) with Fourier collocation in space and 5th-order Runge-Kutta in time. The conservative method uses relaxation to enforce conservation of (3.11b).

### 3.4 Holm-Hone equation

The Holm-Hone equation [30]

$$(4 - 5\partial_x^2 + \partial_x^4)\partial_t u + u\partial_x^5 u + 2(\partial_x u)\partial_x^4 u - 5u\partial_x^3 u - 10(\partial_x u)\partial_x^2 u + 12u\partial_x u = 0, \quad (3.13)$$

$$u(0, x) = u^0(x),$$

with periodic boundary conditions can also be written as

$$\partial_t u + (4I - 5\partial_{x,P}^2 + \partial_{x,P}^4)^{-1} \left( \partial_x (u(4I - 5\partial_x^2 + \partial_x^4)u) + (\partial_x u)(4I - 5\partial_x^2 + \partial_x^4)u \right) = 0, \quad (3.14)$$

where  $(4I - 5\partial_{x,P}^2 + \partial_{x,P}^4)^{-1}$  is the inverse of the elliptic operator  $4I - 5\partial_x^2 + \partial_x^4$  with periodic boundary conditions. The functionals

$$J_1^{\text{HH}}(u) = \int_{x_{\min}}^{x_{\max}} u, \quad (3.15a)$$

$$J_2^{\text{HH}}(u) = \int_{x_{\min}}^{x_{\max}} (4I - \partial_x^2)(I - \partial_x^2)u = \int_{x_{\min}}^{x_{\max}} (4I - 5\partial_x^2 + \partial_x^4)u, \quad (3.15b)$$

$$J_3^{\text{HH}}(u) = \frac{1}{2} \int_{x_{\min}}^{x_{\max}} u(4I - \partial_x^2)(I - \partial_x^2)u = \frac{1}{2} \int_{x_{\min}}^{x_{\max}} (4u^2 + 5(\partial_x u)^2 + (\partial_x^2 u)^2), \quad (3.15c)$$

are invariants of solutions. All of these are conserved by semidiscretizations of the form

$$\partial_t \mathbf{u} = -(4I - 5D_2 + D_4)^{-1} \left( D_1(\mathbf{u}(4I - 5D_2 + D_4)\mathbf{u}) + (D_1 \mathbf{u})(4I - 5D_2 + D_4)\mathbf{u} \right) \quad (3.16)$$

whenever  $D_1, D_2, D_4$  are commuting periodic first-, second-, and fourth-derivative SBP operators with diagonal mass matrix [58].

We use a numerically generated solitary wave solution as initial condition in the periodic domain  $[-40, 40]$ . We apply (3.16) with Fourier collocation differentiation matrices  $D_1, D_2, D_4$  in space and Tsitouras' fifth-order Runge-Kutta method [68] in time, with or without using relaxation to enforce conservation of (3.15c). The error growth is shown in Figure 4 for  $2^9$  nodes and a local error tolerance of  $10^{-9}$ . After an initial transient period, the error of the non-conservative scheme grows quadratically while the corresponding conservative method results in approximately linear error growth.

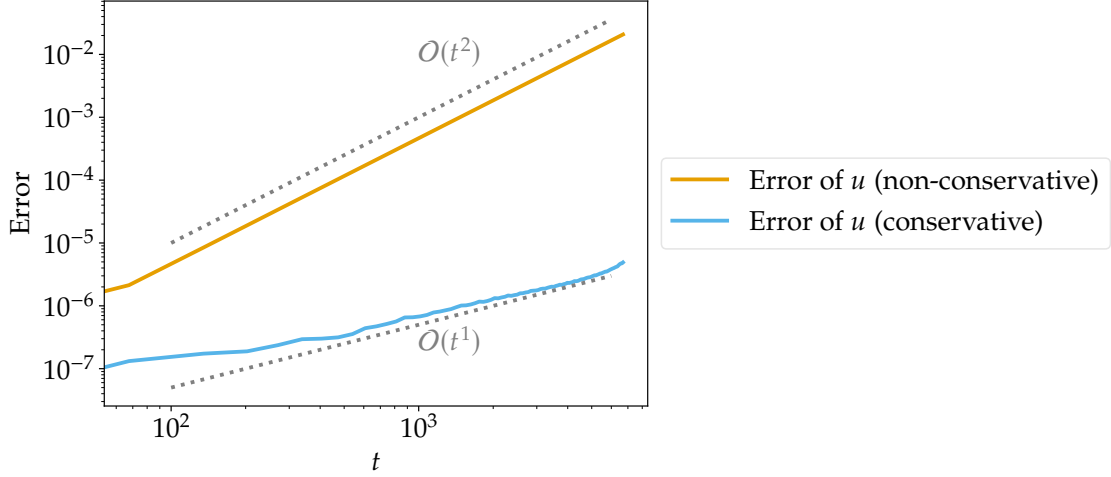


Figure 4: Error growth in time for a numerically generated solitary wave solution of the Holm-Hone equation (3.13), using (3.16) with Fourier collocation in space and 5th-order Runge-Kutta in time. The conservative method uses relaxation to enforce conservation of (3.15c).

### 3.5 BBM-BBM system

The BBM-BBM system [3, 4, 7, 8]

$$\begin{aligned}
 \partial_t \eta(t, x) + \partial_x u(t, x) + \partial_x (\eta(t, x)u(t, x)) - \partial_t \partial_x^2 \eta(t, x) &= 0, \\
 \partial_t u(t, x) + \partial_x \eta(t, x) + \partial_x \frac{u(t, x)^2}{2} - \partial_t \partial_x^2 u(t, x) &= 0, \\
 \eta(0, x) &= \eta^0(x), \\
 u(0, x) &= u^0(x),
 \end{aligned} \tag{3.17}$$

with periodic boundary conditions can also be written as

$$\begin{aligned}
 \partial_t \eta(t, x) + (\mathbf{I} - \partial_{x,p}^2)^{-1} \partial_x (u(t, x) + \eta(t, x)u(t, x)) &= 0, \\
 \partial_t u(t, x) + (\mathbf{I} - \partial_{x,p}^2)^{-1} \partial_x \left( \eta(t, x) + \frac{u(t, x)^2}{2} \right) &= 0,
 \end{aligned} \tag{3.18}$$

where  $(\mathbf{I} - \partial_{x,p}^2)^{-1}$  is the inverse of the elliptic operator  $\mathbf{I} - \partial_x^2$  with periodic boundary conditions. The functionals

$$J_1^{\text{BBM-BBM}}(\eta, u) = \int_{x_{\min}}^{x_{\max}} \eta, \tag{3.19a}$$

$$J_2^{\text{BBM-BBM}}(\eta, u) = \int_{x_{\min}}^{x_{\max}} u, \quad (3.19b)$$

$$J_3^{\text{BBM-BBM}}(\eta, u) = \int_{x_{\min}}^{x_{\max}} (\eta^2 + (1 + \eta)u^2), \quad (3.19c)$$

$$J_4^{\text{BBM-BBM}}(\eta, u) = \int_{x_{\min}}^{x_{\max}} (\eta u + \partial_x \eta \partial_x u) = \int_{x_{\min}}^{x_{\max}} \eta (\mathbf{I} - \partial_x^2) u, \quad (3.19d)$$

are invariants of solutions. The first three of these are conserved by semidiscretizations of the form

$$\begin{aligned} \partial_t \boldsymbol{\eta} + (\mathbf{I} - D_2)^{-1} D_1 (\mathbf{u} + \boldsymbol{\eta} \mathbf{u}) &= \mathbf{0}, \\ \partial_t \mathbf{u} + (\mathbf{I} - D_2)^{-1} D_1 \left( \boldsymbol{\eta} + \frac{1}{2} \mathbf{u}^2 \right) &= \mathbf{0}. \end{aligned} \quad (3.20)$$

whenever  $D_1, D_2$  are commuting periodic first- and second-derivative SBP operators with diagonal mass matrix [58].

We use a numerically generated solitary wave solution as initial condition in the periodic domain  $[-40, 40]$ . We apply (3.20) with Fourier collocation differentiation matrices  $D_1, D_2$  in space and Tsitouras' fifth-order Runge-Kutta method [68] in time, with or without using relaxation to enforce conservation of (3.19c). The error growth is shown in Figure 5 for  $2^8$  nodes and a local error tolerance of  $10^{-5}$ . After an initial transient period, the error of the non-conservative scheme grows quadratically while the corresponding conservative method results in approximately linear error growth. The error of the non-conservative method starts to saturate at  $t \approx 10^4$  since the numerical and reference waves do not overlap anymore, as can be seen in Figure 6. The numerical solutions obtained using the non-conservative method have a visible amplitude error and a significant phase error. In contrast, the conservative method yields numerical solutions that are visually indistinguishable from the reference solution.

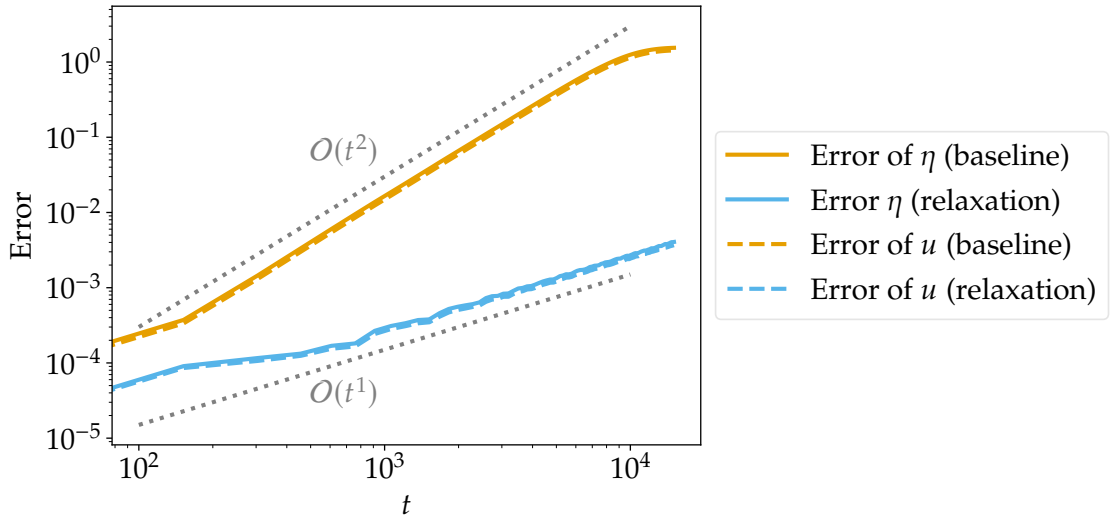


Figure 5: Error growth in time for a numerically generated solitary wave solution of the BBM-BBM system (3.17), using (3.20) with Fourier collocation in space and 5th-order Runge-Kutta in time. The conservative method uses relaxation to enforce conservation of (3.19c).

**Remark 3.1.** It is also possible to construct semidiscretizations of the BBM-BBM system that conserve the quadratic functional (3.19d) instead of the cubic energy (3.19c), e.g. the

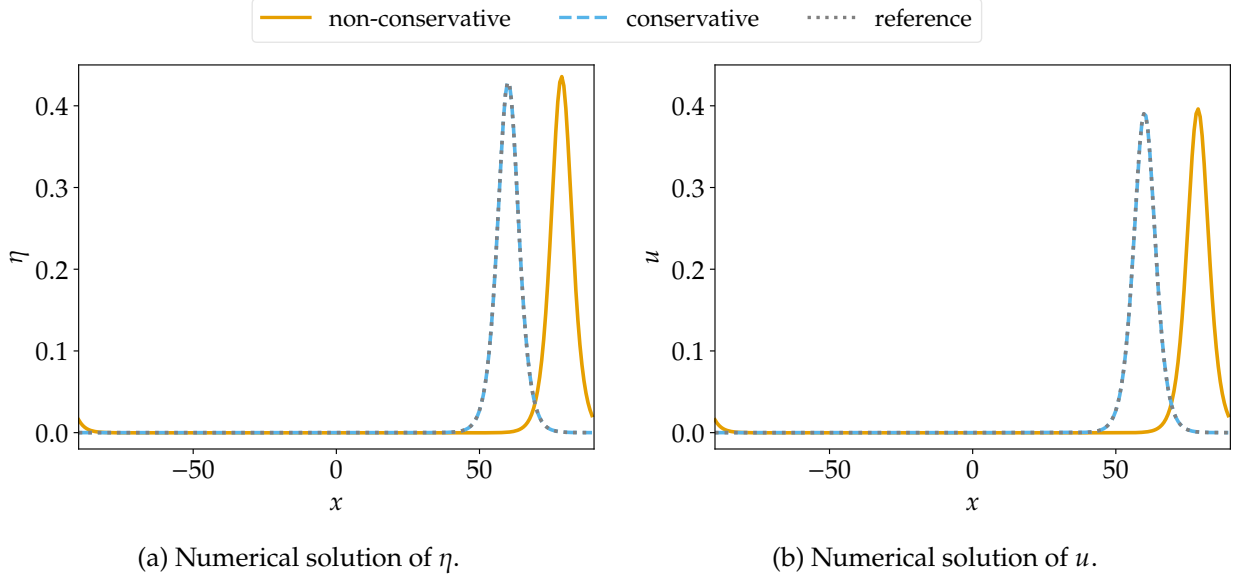


Figure 6: Numerical solutions at the final time for a numerically generated solitary wave solution of the BBM-BBM system (3.17) using relaxation methods conserving the energy (3.19c).

standard Galerkin method [41] or SBP methods using the split form

$$\begin{aligned} \partial_t \boldsymbol{\eta} + (\mathbf{I} - D_2)^{-1} D_1(\mathbf{u} + \boldsymbol{\eta} \mathbf{u}) &= \mathbf{0}, \\ \partial_t \mathbf{u} + (\mathbf{I} - D_2)^{-1} (D_1 \boldsymbol{\eta} + \mathbf{u} D_1 \mathbf{u}) &= \mathbf{0}; \end{aligned} \quad (3.21)$$

see Theorem 3.2 below. The error growth in time using this method for the test problem above is visually indistinguishable from that shown for the method (3.20). In particular, the error of the associated conservative method grows linearly in time while the error of the non-conservative method grows quadratically.  $\triangleleft$

**Theorem 3.2.** *If  $D_1$  is a periodic first-derivative SBP operator and  $D_2$  is a periodic second-derivative SBP operator with diagonal mass matrix, then the semidiscretization (3.21) conserves the linear invariants (3.19a) and (3.19b) as well as the quadratic invariant (3.19d) of (3.18).*

*Proof.* Using  $\mathbf{1}^T M (\mathbf{I} - D_2)^{-1} = \mathbf{1}^T M$  [58, Lemma 2.28] and  $\mathbf{1}^T M D_1 = \mathbf{0}^T$  [58, Lemma 2.27] results in

$$\mathbf{1}^T M \partial_t \boldsymbol{\eta} = -\mathbf{1}^T M (\mathbf{I} - D_2)^{-1} D_1(\mathbf{u} + \boldsymbol{\eta} \mathbf{u}) = 0. \quad (3.22)$$

Applying the SBP property (2.2) additionally and using that  $M$  is diagonal yields

$$\mathbf{1}^T M \partial_t \mathbf{u} = -\mathbf{1}^T M (\mathbf{I} - D_2)^{-1} (D_1 \boldsymbol{\eta} + \mathbf{u} D_1 \mathbf{u}) = -\mathbf{u}^T M D_1 \mathbf{u} = 0. \quad (3.23)$$

Finally, similar arguments based on the symmetry of  $\mathbf{I} - D_2$  with respect to the mass matrix  $M$  lead to

$$\begin{aligned} \partial_t J_4^{\text{BBM-BBM}}(\boldsymbol{\eta}, \mathbf{u}) &= \mathbf{u}^T M (\mathbf{I} - D_2) \partial_t \boldsymbol{\eta} + \boldsymbol{\eta}^T M (\mathbf{I} - D_2) \partial_t \mathbf{u} \\ &= -\mathbf{u}^T M D_1(\mathbf{u} + \boldsymbol{\eta} \mathbf{u}) - \boldsymbol{\eta}^T M (D_1 \boldsymbol{\eta} + \mathbf{u} D_1 \mathbf{u}) = 0. \end{aligned} \quad (3.24) \quad \square$$

## 4 A linear dispersive equation

As alluded to in the introduction, nonlinearity is an important condition to observe different behaviors of the error growth in time. To demonstrate that, we consider the

linear dispersive equation

$$\begin{aligned} (\mathbf{I} - \partial_x^2) \partial_t u(t, x) + \partial_x u(t, x) &= 0, & t \in (0, T), x \in (x_{\min}, x_{\max}), \\ u(0, x) &= u^0(x), & x \in [x_{\min}, x_{\max}], \end{aligned} \quad (4.1)$$

with periodic boundary conditions. The functionals

$$J_1^{\text{lin}}(u) = \int_{x_{\min}}^{x_{\max}} u, \quad (4.2a)$$

$$J_2^{\text{lin}}(u) = \int_{x_{\min}}^{x_{\max}} (u^2 + (\partial_x u)^2) = \int_{x_{\min}}^{x_{\max}} u(\mathbf{I} - \partial_x^2)u, \quad (4.2b)$$

are invariants of solutions of (4.1), which are conserved by semidiscretizations of the form

$$\partial_t \mathbf{u} + (\mathbf{I} - D_2)^{-1} D_1 \mathbf{u} = \mathbf{0}. \quad (4.3)$$

**Theorem 4.1.** *If  $D_1$  is a periodic first-derivative SBP operator and  $D_2$  is a periodic second-derivative SBP operator, then the semidiscretization (4.3) conserves the invariants (4.2) of (4.1).*

*Proof.* Using  $\mathbf{1}^T M(\mathbf{I} - D_2)^{-1} = \mathbf{1}^T M$  [58, Lemma 2.28] and  $\mathbf{1}^T M D_1 = \mathbf{0}^T$  [58, Lemma 2.27] results in

$$\mathbf{1}^T M \partial_t \mathbf{u} = -\mathbf{1}^T M (\mathbf{I} - D_2)^{-1} D_1 \mathbf{u} = 0. \quad (4.4)$$

Using the symmetry of  $\mathbf{I} - D_2$  with respect to the mass matrix  $M$  and applying the SBP property (2.2) results in

$$\partial_t J_2^{\text{lin}}(\mathbf{u}) = 2\mathbf{u}^T M (\mathbf{I} - D_2) \partial_t \mathbf{u} = -2\mathbf{u}^T M D_1 \mathbf{u} = -\mathbf{u}^T M D_1 \mathbf{u} + \mathbf{u}^T D_1^T M \mathbf{u} = 0. \quad (4.5)$$

□

Numerical result for the analytical solution

$$u(t, x) = \sin(\pi(x - ct)), \quad c = \frac{1}{1 + 4\pi^2}, \quad (4.6)$$

in the domain  $[x_{\min}, x_{\max}] = [-1, 1]$  are shown in Figure 7. The spatial semidiscretization using a Fourier pseudospectral method with  $N = 2^6$  nodes is integrated in time with the fifth-order accurate Runge-Kutta method of [68] and a tolerance of  $10^{-5}$ . While the conservative method has a significantly reduced amplitude error, the phase error of the conservative and non-conservative methods are visually indistinguishable. Consequently, the error growth rate in time for both methods is linear. This is in accordance with analytical results available for other linear equations such as hyperbolic systems with constant coefficients in periodic domains; for these equations, the error can also be bounded in time if non-periodic domains are used and the boundary conditions are imposed appropriately [36, 43, 46, 47].

## 5 The variable-coefficient $p$ -system

The examples in Section 3 all involve dispersive nonlinear wave equations with constant coefficients. The results there are in line with the results available in the literature, all

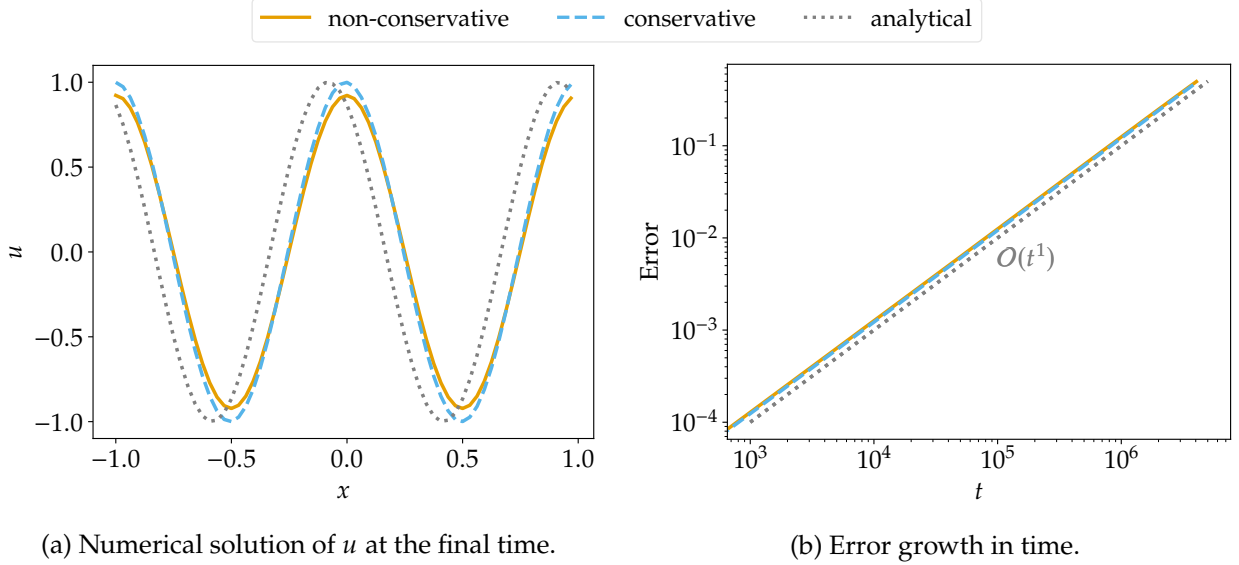


Figure 7: Numerical results for the linear dispersive equation (4.1) using relaxation methods conserving the energy (4.2b).

of which involve similar dispersive nonlinear wave equations. We now turn to a very different kind of example that demonstrates the generality of the behavior in question. Specifically, we study a system of nonlinear first-order hyperbolic conservation laws with spatially-varying coefficients. This system has no dispersive terms, and in a strict sense has no traveling wave solutions. It has been observed to possess solutions (known as “stegotons”) that are similar to solitary waves, although they change shape periodically in time; see [38].

Specifically, we investigate the behavior of numerical solutions to the first-order system

$$\begin{aligned} \partial_t \varepsilon(t, x) - \partial_x u(t, x) &= 0 \\ \varrho(x) \partial_t u(t, x) - \partial_x \sigma(\varepsilon(t, x), x) &= 0, \end{aligned} \quad (5.1)$$

where  $u$  is the velocity,  $\varrho$  the prescribed density,  $\varepsilon$  the strain, and

$$\sigma(\varepsilon, x) = \exp(K(x)\varepsilon) - 1 \quad (5.2)$$

the stress [38]. Here we have used notation corresponding to elasticity, but the same system arises in Lagrangian gas dynamics and is referred to as the  $p$ -system. The energy

$$\int E(u(t, x), \varepsilon(t, x), x) dx, \quad E(u, \varepsilon, x) = \frac{1}{2} \varrho(x) u^2 + \int_0^\varepsilon \sigma(s, x) ds \quad (5.3)$$

is conserved for strong solutions of (5.1). Generically, solutions of this system give rise to discontinuities (shocks) and a theory of weak solutions must be invoked. However, with appropriate initial data and periodic variation of the PDE coefficients, solutions appear to be regular for all time and the energy (5.3) is conserved [33].

A straightforward application of an SBP operator  $D_1$  in a periodic domain results in the semidiscretization

$$\begin{aligned} \partial_t \boldsymbol{\varepsilon} &= D_1 \mathbf{u}, \\ \partial_t \mathbf{u} &= \boldsymbol{\varrho}^{-1} D_1 \boldsymbol{\sigma}, \end{aligned} \quad (5.4)$$

where  $\boldsymbol{\sigma}$  and the division by  $\boldsymbol{\varrho}$  are evaluated pointwise.

**Theorem 5.1.** *Let  $D_1$  be a periodic SBP first-derivative operator with diagonal mass matrix  $M$ . Then the semidiscretization (5.4) conserves the total mass of  $\varepsilon$ , the total mass of  $\varrho u$ , and the total energy  $\eta = \int E$ .*

*Proof.* For a periodic SBP operator, the rate of change of the total masses is

$$\begin{aligned}\partial_t \mathbf{1}^T M \boldsymbol{\varepsilon} &= \mathbf{1}^T M D_1 \mathbf{u} = \mathbf{0}, \\ \partial_t \mathbf{1}^T M \varrho \mathbf{u} &= \mathbf{1}^T M D_1 \boldsymbol{\sigma} = \mathbf{0}.\end{aligned}\tag{5.5}$$

Furthermore,

$$\partial_t \eta = \partial_t \mathbf{1}^T M \boldsymbol{\eta} = \frac{1}{2} \partial_t \mathbf{1}^T M \varrho \mathbf{u}^2 + \partial_t \mathbf{1}^T M \boldsymbol{\Sigma},\tag{5.6}$$

where  $\boldsymbol{\Sigma} = \int_0^\varepsilon \sigma(s, x) ds$ . Hence,

$$\begin{aligned}\partial_t \eta &= \mathbf{1}^T M \varrho \mathbf{u} \partial_t \mathbf{u} + \mathbf{1}^T M \sigma \partial_t \boldsymbol{\varepsilon} = \mathbf{1}^T M \mathbf{u} D_1 \boldsymbol{\sigma} + \mathbf{1}^T M \sigma D_1 \mathbf{u} \\ &= \mathbf{u}^T M D_1 \boldsymbol{\sigma} + \boldsymbol{\sigma}^T M D_1 \mathbf{u} = 0,\end{aligned}\tag{5.7}$$

where we have used that the mass matrix is diagonal.  $\square$

We use smooth coefficients given by

$$\varrho(x) = \frac{5}{2} - \frac{3}{2} \sin(2\pi x), \quad K(x) = \frac{5}{2} - \frac{3}{2} \sin(2\pi x),$$

in the domain  $[0, 20]$ . To study the error growth in time, we construct a stegoton solution numerically using Clawpack [14, 34, 35, 40] as follows. We start with a zero initial condition and a left boundary condition given by

$$\begin{aligned}\varepsilon(0, t) &= 0, \\ u(0, t) &= \begin{cases} -0.1 [1 + \cos(t_0 \pi)], & \text{if } |t_0| \leq 1, \\ 0, & \text{otherwise,} \end{cases}\end{aligned}$$

where  $t_0 = \frac{t-2.5}{2.5}$ . This corresponds to a moving wall that generates a pulse that eventually becomes a train of stegotons. We solve this problem to a late time (so that the stegotons are well separated) on a highly-refined grid, and then isolate the first resulting stegoton. For more details see [57].

Next, we use the numerically constructed single-stegoton solution as initial condition. We apply an energy-conservative Fourier pseudospectral semidiscretization (5.4) with  $2^8$  nodes. We solve the resulting ODE system using the fifth-order Runge-Kutta method of [68] with adaptive time stepping and a tolerance of  $10^{-6}$ . The error growth is shown in Figure 8 for solutions obtained with relaxation (conservative) and without relaxation (non-conservative). After an initial transient period, the error of the non-conservative scheme grows quadratically while the corresponding conservative method results in approximately linear error growth. The error of the non-conservative method starts to saturate at  $t \approx 10^4$  since the numerical and reference waves do not overlap anymore, as can be seen in Figure 9. The numerical solutions obtained using the non-conservative method have a clearly visible phase error. In addition, the shape of the numerical solutions is deformed, in particular for  $u$ . In contrast, the phase error of the conservative method is negligible. Nevertheless, the shape of the numerical solutions has changed a bit over these very long-time simulations, and small oscillations have appeared in the tails of the solitary wave.

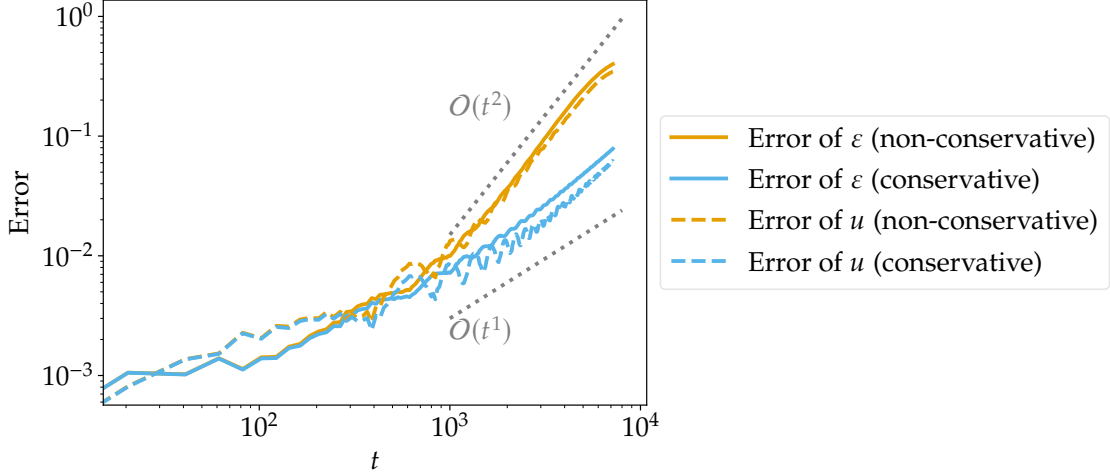


Figure 8: Error growth in time for a numerically generated stegoton solution of the variable-coefficient  $p$ -system (5.1), using (5.4) with Fourier collocation in space and fifth-order Runge-Kutta in time. The conservative method uses relaxation to enforce conservation of (5.3).

## 6 The shallow water equations

We now turn to the shallow water equations in two space dimensions. Like the last example, this is a first-order hyperbolic system whose solutions generically develop shock discontinuities. As with the last example, for appropriate initial data and varying bathymetry, numerical experiments suggest that solitary wave solutions exist [39]. Nevertheless, this example differs in important ways from all the preceding ones and from all the results available in the literature on error growth for dispersive nonlinear waves. It is a two-dimensional system, and its solitary wave solutions have a two-dimensional structure. Aside from the theoretical complication this involves, it also imposes a practical challenge. Since the exact form of the solitary wave solutions is not known, we will need to compute an approximate solitary wave initial condition, as we did in Section 5. However, in this case we will not be able to exhaustively resolve the solution and we expect that resulting initial condition will be close to, but still different from, a solitary wave.

The shallow water equations in two space dimensions with variable bathymetry  $b(x, y)$  are

$$\begin{aligned} \partial_t h + \partial_x(hv_x) + \partial_y(hv_y) &= 0, \\ \partial_t(hv_x) + \partial_x(hv_x^2 + \frac{1}{2}gh^2) + \partial_y(hv_xv_y) &= -gh\partial_x b, \\ \partial_t(hv_y) + \partial_x(hv_xv_y) + \partial_y(hv_y^2 + \frac{1}{2}gh^2) &= -gh\partial_y b, \end{aligned} \quad (6.1)$$

where  $h(x, y, t)$  is the water height and  $v_x(x, y, t), v_y(x, y, t)$  are the  $x$ - and  $y$ -components of velocity, respectively. The conserved energy is

$$E = \frac{1}{2}(hv^2 + gh^2) + ghb. \quad (6.2)$$

A two-parameter family of well-balanced, energy-conservative semidiscretizations of the shallow water equations with variable bathymetry was presented in [50, 53]. The semidiscretization

$$\partial_t \mathbf{h} = -D_{1,x} \mathbf{h} v_x - D_{1,y} \mathbf{h} v_y, \quad (6.3a)$$



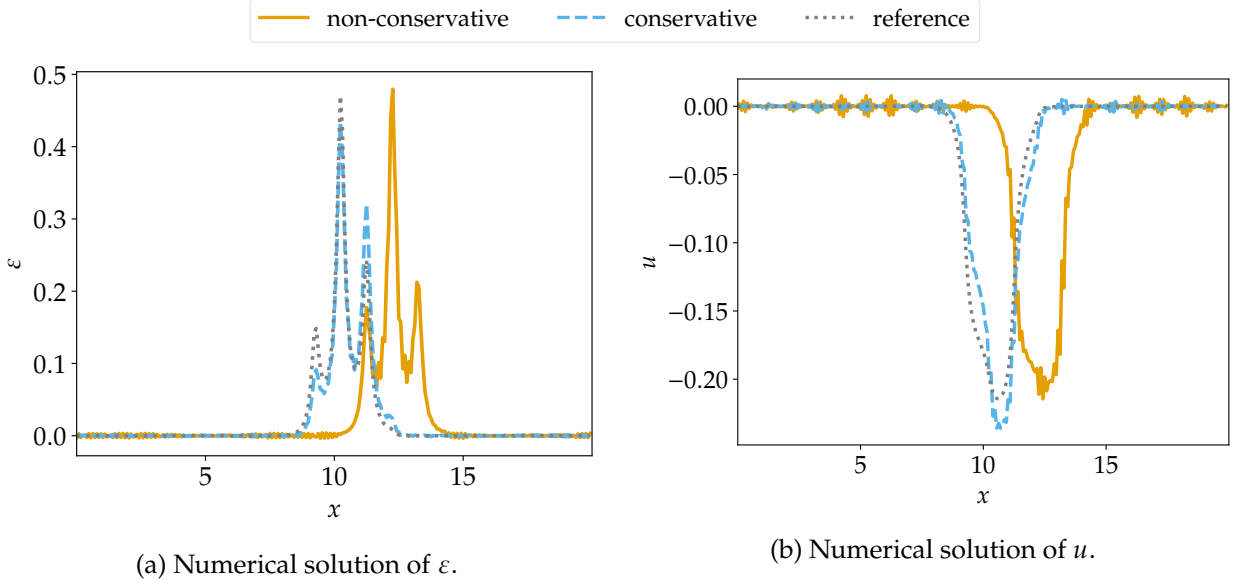


Figure 9: Numerical solutions at the final time for a numerically generated stegoton solution of the variable-coefficient  $p$ -system (5.1). The conservative solution is visually indistinguishable from the reference solution.

$$\partial_t h v_x = -\frac{1}{2} D_{1,x} h v_x^2 - \frac{1}{2} h v_x D_{1,x} v_x - \frac{1}{2} v_x D_{1,x} h v_x \quad (6.3b)$$

$$-\frac{1}{2} D_{1,y} h v_x v_y - \frac{1}{2} h v_x D_{1,y} v_y - \frac{1}{2} v_y D_{1,y} h v_x - g h D_{1,x} (h + b), \quad (6.3c)$$

$$\partial_t h v_y = -\frac{1}{2} D_{1,x} h v_x v_y - \frac{1}{2} h v_y D_{1,x} v_x - \frac{1}{2} v_x D_{1,x} h v_y \quad (6.3d)$$

$$-\frac{1}{2} D_{1,y} h v_y^2 - \frac{1}{2} h v_y D_{1,y} v_y - \frac{1}{2} v_y D_{1,y} h v_y - g h D_{1,y} (h + b). \quad (6.3e)$$

is a member of this family and was presented earlier in [26, 70], see also [23] for related methods.

In the following, we use the gravitational constant  $g = 9.8$  and the smooth bottom topography

$$b(x, y) = \frac{1}{4} - \frac{1}{4} \sin(2\pi y) \quad (6.4)$$

in the domain  $[0, 20] \times [-0.5, 0.5]$  with periodic boundary conditions. To study the error growth in time, we construct a solitary wave solution as follows. Based on [39], we start with an initial condition given by

$$h(x, y) + b(x, y) = \eta^* + A \exp\left(-\frac{x^2}{4}\right), \quad h v_x(x, y) = h v_y(x, y) = 0,$$

where  $\eta^* = 0.75$  and  $A = 5 \times 10^{-2}$ . After propagating the initial condition up to a final time of  $t = 340$ , we obtain a train of solitary waves, from which we isolate the largest wave. For more details see [57].

Next, we use the numerically constructed wave as initial condition for an energy-conservative Fourier pseudospectral discretization (6.3) with  $2^{10}$  nodes in  $x$  and  $2^6$  nodes in  $y$ . We solve the resulting ODE using the fifth-order Runge-Kutta method of [68] with adaptive time stepping and a tolerance of  $10^{-6}$ . The error growth is shown in Figure 10.

In contrast to the examples considered so far, the error growth rates of both methods are sublinear. In agreement with previous results, the error of the conservative methods still grows significantly slower, resulting in an error at the final time (after 15 periods) that is approximately an order of magnitude smaller.

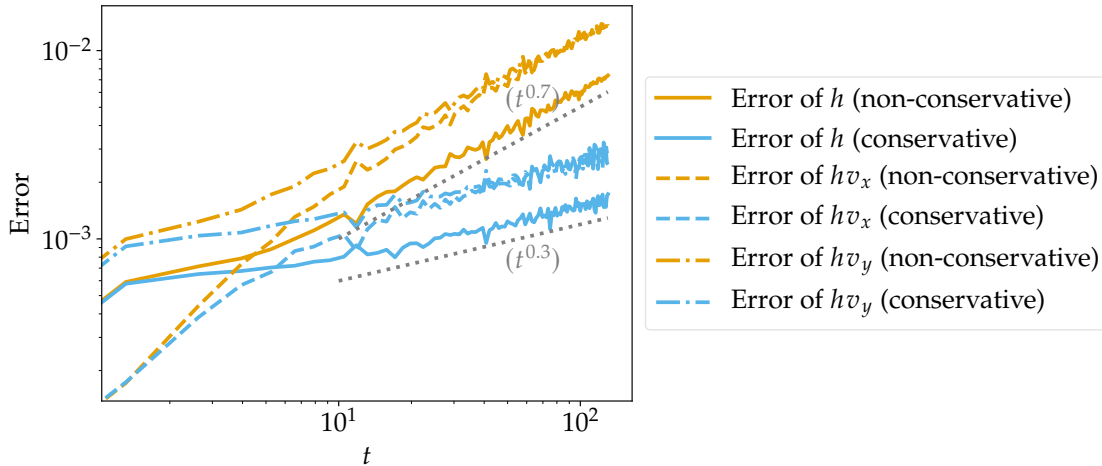


Figure 10: Error growth in time for a numerically generated solitary wave solution of the shallow-water equations (6.1).

Snapshots of the numerical solutions at the final time are shown in Figures 11 and 12. The conservative method advects the profiles of the perturbations well, resulting in a numerical solution that is visually nearly indistinguishable from the initial profile. In contrast, the non-conservative method results in a slightly visible phase error. In addition, signs of nonlinear instabilities in the form of high-frequency oscillations start to manifest in the y-momentum and in reduced form also in the x-momentum and the total water height.

Possible reasons for error growth rates that are not linear/quadratic stem from differences relative to the other equations studied so far: this system is two-dimensional, there are no known exact solitary wave solutions, and the computed initial solitary wave is still affected by small numerical errors due to the cost of fully resolving the wave in two dimensions.

Although these numerical results presented for the shallow water equations do not match the linear/quadratic error growth rates of the other examples discussed previously, they still show the usefulness of conservative methods. In the current implementation, the CPU time of the conservative and non-conservative method are comparable while the accuracy differs by an order of magnitude. To obtain similarly accurate solutions using the non-conservative method would require an increased space/time resolution and hence more computational resources.

## 7 Summary and conclusions

We have studied the error growth in time of numerical solitary wave solutions of several systems of PDEs, focusing on the difference in behavior between conservative and non-conservative methods. In all cases, the general pattern is the same: conservative methods exhibit linear error growth, while non-conservative methods exhibit quadratic

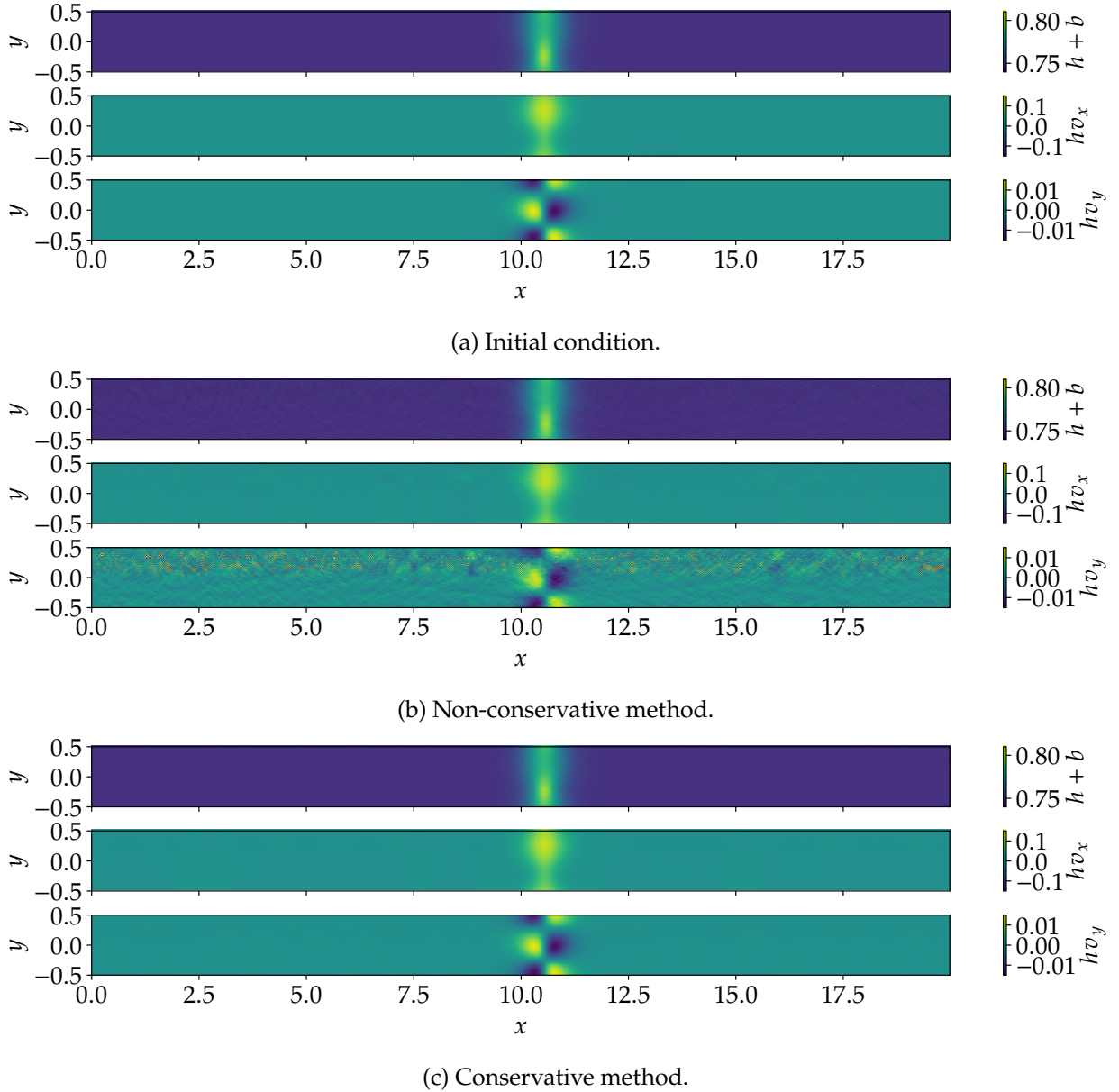


Figure 11: Snapshots of numerical solutions for a numerically generated solitary wave solution of the shallow-water equations (6.1).

error growth. As one might expect based on this, the magnitude of the error itself is also much smaller for conservative methods.

We have shown that this phenomenon extends to a wide range of dispersive nonlinear wave equations, and that this behavior seems to arise when *any* nonlinear invariant is conserved, even if it is not quadratic (see Section 3.5). Furthermore, we have shown that this behavior extends to other classes of equations, including the  $p$ -system example in Section 5. This is remarkable in that the equations in question are non-dispersive and the solutions are not traveling waves in the usual sense. Nevertheless, a similar advantage is obtained by using a conservative discretization.

This suggests that conservative methods may be much more efficient for solving wave problems that possess one or more conserved functionals. Efficiency depends also on the cost of the method, which we have not focused on here. In most previous works related to this phenomenon, energy conservation was achieved through the use of fully-

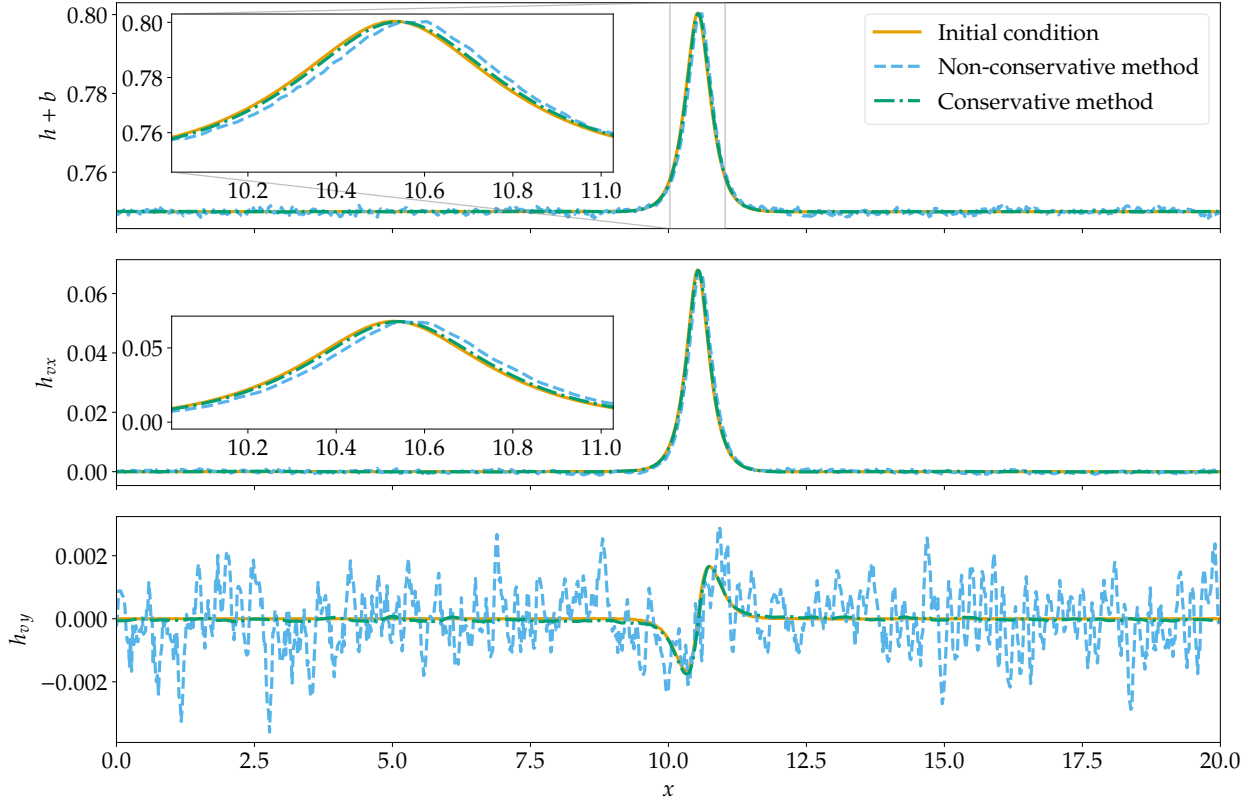


Figure 12: Slices at  $y \approx -0.26$  of the numerical solutions shown in Figure 11.

implicit Runge-Kutta time integration. With the relaxation Runge-Kutta approach, we can instead employ essentially explicit relaxation Runge-Kutta methods for non-stiff spatial discretizations, and diagonally implicit or linearly implicit (Rosenbrock) methods for stiff problems. These incur only a very small additional cost per time step (in order to solve a scalar algebraic equation). For the methods we have compared here, at least, the conservative approach using relaxation is much more efficient (in terms of computational cost for a given level of error) than the corresponding non-conservative method.

It is natural to ask whether the behavior studied here can be observed for more general solutions (not consisting of a single traveling wave). This is the subject of ongoing work, and initial tests suggest a complex variety of behaviors. Nevertheless, these tests show that conservative methods are consistently much more accurate than their non-conservative counterparts.

## Acknowledgments

Research reported in this publication was supported by the King Abdullah University of Science and Technology (KAUST).

## References

- [1] R. Abgrall, J. Nordström, P. Öffner, and S. Tokareva. “Analysis of the SBP-SAT Stabilization for Finite Element Methods Part I: Linear problems.” In: *Journal of*

- Scientific Computing* 85.2 (2020), pp. 1–29. DOI: 10.1007/s10915-020-01349-z. arXiv: 1912.08108 [math.NA].
- [2] G. Alefeld, F. A. Potra, and Y. Shi. “Algorithm 748: Enclosing Zeros of Continuous Functions.” In: *ACM Transactions on Mathematical Software (TOMS)* 21.3 (1995), pp. 327–344. DOI: 10.1145/210089.210111.
  - [3] D. C. Antonopoulos, V. A. Dougalis, and D. E. Mitsotakis. “Initial-boundary-value problems for the Bona-Smith family of Boussinesq systems.” In: *Advances in Differential Equations* 14.1/2 (2009), pp. 27–53.
  - [4] D. C. Antonopoulos, V. A. Dougalis, and D. E. Mitsotakis. “Numerical solution of Boussinesq systems of the Bona-Smith family.” In: *Applied Numerical Mathematics* 60.4 (2010), pp. 314–336. DOI: 10.1016/j.apnum.2009.03.002.
  - [5] A Araújo and A. Durán. “Error propagation in the numerical integration of solitary waves. The regularized long wave equation.” In: *Applied Numerical Mathematics* 36.2-3 (2001), pp. 197–217. DOI: 10.1016/S0168-9274(99)00148-8.
  - [6] J. Bezanson, A. Edelman, S. Karpinski, and V. B. Shah. “Julia: A Fresh Approach to Numerical Computing.” In: *SIAM Review* 59.1 (2017), pp. 65–98. DOI: 10.1137/141000671. arXiv: 1411.1607 [cs.MS].
  - [7] J. L. Bona, M. Chen, and J.-C. Saut. “Boussinesq Equations and Other Systems for Small-Amplitude Long Waves in Nonlinear Dispersive Media. I: Derivation and Linear Theory.” In: *Journal of Nonlinear Science* 12.4 (2002). DOI: 10.1007/s00332-002-0466-4.
  - [8] J. L. Bona, M. Chen, and J.-C. Saut. “Boussinesq equations and other systems for small-amplitude long waves in nonlinear dispersive media: II. The nonlinear theory.” In: *Nonlinearity* 17.3 (2004), p. 925. DOI: 10.1088/0951-7715/17/3/010.
  - [9] M. Calvo, M. Laburta, J. I. Montijano, and L. Rández. “Error growth in the numerical integration of periodic orbits.” In: *Mathematics and Computers in Simulation* 81.12 (2011), pp. 2646–2661. DOI: 10.1016/j.matcom.2011.05.007.
  - [10] R. Camassa and D. D. Holm. “An integrable shallow water equation with peaked solitons.” In: *Physical Review Letters* 71.11 (1993), p. 1661. DOI: 10.1103/PhysRevLett.71.1661.
  - [11] B Cano and J. M. Sanz-Serna. “Error growth in the numerical integration of periodic orbits, with application to Hamiltonian and reversible systems.” In: *SIAM Journal on Numerical Analysis* 34.4 (1997), pp. 1391–1417. DOI: 10.1137/S0036142995281152.
  - [12] B Cano and J. Sanz-Serna. “Error growth in the numerical integration of periodic orbits by multistep methods, with application to reversible systems.” In: *IMA Journal of Numerical Analysis* 18.1 (1998), pp. 57–75. DOI: 10.1093/imanum/18.1.57.
  - [13] T. Chen and C.-W. Shu. “Review of entropy stable discontinuous Galerkin methods for systems of conservation laws on unstructured simplex meshes.” In: *CSIAM Transactions on Applied Mathematics* 1.1 (2020), pp. 1–52. DOI: 10.4208/csiam-am.2020-0003.
  - [14] Clawpack Development Team. *Clawpack software*. Version 5.6.1. 2019. DOI: 10.5281/zenodo.3528429. URL: <http://www.clawpack.org>.
  - [15] J De Frutos and J. M. Sanz-Serna. “Accuracy and conservation properties in numerical integration: the case of the Korteweg-de Vries equation.” In: *Numerische Mathematik* 75.4 (1997), pp. 421–445. DOI: 10.1007/s002110050247.

- [16] A. Degasperis, D. D. Holm, and A. N. Hone. “A new integrable equation with peakon solutions.” In: *Theoretical and Mathematical Physics* 133.2 (2002), pp. 1463–1474. doi: 10.1023/A:1021186408422.
- [17] K. Dekker and J. G. Verwer. *Stability of Runge-Kutta methods for stiff nonlinear differential equations*. Vol. 2. CWI Monographs. Amsterdam: North-Holland, 1984.
- [18] A. Durán and M. López-Marcos. “Conservative numerical methods for solitary wave interactions.” In: *Journal of Physics A: Mathematical and General* 36.28 (2003), p. 7761. doi: 10.1088/0305-4470/36/28/306.
- [19] A. Durán and M. López-Marcos. “Numerical behaviour of stable and unstable solitary waves.” In: *Applied Numerical Mathematics* 42.1-3 (2002), pp. 95–116. doi: 10.1016/S0168-9274(01)00144-1.
- [20] A. Durán and J. M. Sanz-Serna. “The numerical integration of relative equilibrium solutions. Geometric theory.” In: *Nonlinearity* 11.6 (1998), p. 1547. doi: 10.1088/0951-7715/11/6/008.
- [21] A. Durán and J. Sanz-Serna. “The numerical integration of relative equilibrium solutions. The nonlinear Schrödinger equation.” In: *IMA Journal of Numerical Analysis* 20.2 (2000), pp. 235–261. doi: 10.1093/imanum/20.2.235.
- [22] D. C. D. R. Fernández, J. E. Hicken, and D. W. Zingg. “Review of summation-by-parts operators with simultaneous approximation terms for the numerical solution of partial differential equations.” In: *Computers & Fluids* 95 (2014), pp. 171–196. doi: 10.1016/j.compfluid.2014.02.016.
- [23] U. S. Fjordholm, S. Mishra, and E. Tadmor. “Well-balanced and energy stable schemes for the shallow water equations with discontinuous topography.” In: *Journal of Computational Physics* 230.14 (2011), pp. 5587–5609. doi: 10.1016/j.jcp.2011.03.042.
- [24] B. Fornberg. “On a Fourier method for the integration of hyperbolic equations.” In: *SIAM Journal on Numerical Analysis* 12.4 (1975), pp. 509–528. doi: 10.1137/0712040.
- [25] G. J. Gassner. “A Skew-Symmetric Discontinuous Galerkin Spectral Element Discretization and Its Relation to SBP-SAT Finite Difference Methods.” In: *SIAM Journal on Scientific Computing* 35.3 (2013), A1233–A1253. doi: 10.1137/120890144.
- [26] G. J. Gassner, A. R. Winters, and D. A. Kopriva. “A well balanced and entropy conservative discontinuous Galerkin spectral element method for the shallow water equations.” In: *Applied Mathematics and Computation* 272 (2016), pp. 291–308. doi: 10.1016/j.amc.2015.07.014.
- [27] G. J. Gassner, A. R. Winters, and D. A. Kopriva. “Split Form Nodal Discontinuous Galerkin Schemes with Summation-By-Parts Property for the Compressible Euler Equations.” In: *Journal of Computational Physics* 327 (2016), pp. 39–66. doi: 10.1016/j.jcp.2016.09.013.
- [28] J. E. Hicken. “Entropy-stable, high-order summation-by-parts discretizations without interface penalties.” In: *Journal of Scientific Computing* 82.2 (2020), p. 50. doi: 10.1007/s10915-020-01154-8.
- [29] J. E. Hicken, D. C. D. R. Fernández, and D. W. Zingg. “Multidimensional Summation-By-Parts Operators: General Theory and Application to Simplex Elements.” In: *SIAM Journal on Scientific Computing* 38.4 (2016), A1935–A1958. doi: 10.1137/15M1038360.

- [30] D. D. Holm and A. N. Hone. “Nonintegrability of a fifth-order equation with integrable two-body dynamics.” In: *Theoretical and Mathematical Physics* 137.1 (2003), pp. 1459–1471. DOI: 10.1023/A:1026060924520.
- [31] J. D. Hunter. “Matplotlib: A 2D graphics environment.” In: *Computing in Science & Engineering* 9.3 (2007), pp. 90–95. DOI: 10.1109/MCSE.2007.55.
- [32] D. I. Ketcheson. “Relaxation Runge-Kutta Methods: Conservation and Stability for Inner-Product Norms.” In: *SIAM Journal on Numerical Analysis* 57.6 (2019), pp. 2850–2870. DOI: 10.1137/19M1263662. arXiv: 1905.09847 [math.NA].
- [33] D. I. Ketcheson and R. J. LeVeque. “Shock Dynamics in Layered Periodic Media.” In: *Communications in Mathematical Sciences* 10.3 (2012), pp. 859–874. DOI: 10.4310/CMS.2012.v10.n3.a7. arXiv: 1105.2892 [math-ph].
- [34] D. I. Ketcheson, K. Mandli, A. J. Ahmadi, A. Alghamdi, M. Quezada de Luna, M. Parsani, M. G. Knepley, and M. Emmett. “PyClaw: Accessible, extensible, scalable tools for wave propagation problems.” In: *SIAM Journal on Scientific Computing* 34.4 (2012), pp. C210–C231. DOI: 10.1137/110856976.
- [35] D. I. Ketcheson, M. Parsani, and R. J. LeVeque. “High-order wave propagation algorithms for hyperbolic systems.” In: *SIAM Journal on Scientific Computing* 35.1 (2013), A351–A377. DOI: 10.1137/110830320.
- [36] D. A. Kopriva, J. Nordström, and G. J. Gassner. “Error boundedness of discontinuous Galerkin spectral element approximations of hyperbolic problems.” In: *Journal of Scientific Computing* 72.1 (2017), pp. 314–330. DOI: 10.1007/s10915-017-0358-2.
- [37] H.-O. Kreiss and J. Oliger. “Comparison of accurate methods for the integration of hyperbolic equations.” In: *Tellus* 24.3 (1972), pp. 199–215. DOI: 10.3402/tellusa.v24i3.10634.
- [38] R. J. LeVeque and D. H. Yong. “Solitary waves in layered nonlinear media.” In: *SIAM Journal on Applied Mathematics* 63.5 (2003), pp. 1539–1560. DOI: 10.1137/S0036139902408151.
- [39] M. Quezada de Luna and D. I. Ketcheson. *Solitary water waves created by variations in bathymetry*. 2019. arXiv: 1907.07094v2 [math.NA].
- [40] K. T. Mandli, A. J. Ahmadi, M. Berger, D. Calhoun, D. L. George, Y. Hadjimichael, D. I. Ketcheson, G. I. Lemoine, and R. J. LeVeque. “Clawpack: building an open source ecosystem for solving hyperbolic PDEs.” In: *PeerJ Computer Science* 2 (2016), e68. DOI: 10.7717/peerj-cs.68.
- [41] D. Mitsotakis, H. Ranocha, D. I. Ketcheson, and E. Süli. *A conservative fully-discrete numerical method for the regularised shallow water wave equations*. Accepted in *SIAM Journal on Scientific Computing*. Jan. 2021. arXiv: 2009.09641 [math.NA].
- [42] E. Momoniat. “A modified equation approach to selecting a nonstandard finite difference scheme applied to the regularized long wave equation.” In: *Abstract and Applied Analysis* 2014 (2014). DOI: 10.1155/2014/754543.
- [43] J. Nordström. “Error Bounded Schemes for Time-Dependent Hyperbolic Problems.” In: *SIAM Journal on Scientific Computing* 30.1 (2007), pp. 46–59. DOI: 10.1137/060654943.
- [44] J. Nordström and M. Björck. “Finite volume approximations and strict stability for hyperbolic problems.” In: *Applied Numerical Mathematics* 38.3 (2001), pp. 237–255. DOI: 10.1016/S0168-9274(01)00027-7.

- [45] J. Nordström, K. Forsberg, C. Adamsson, and P. Eliasson. “Finite volume methods, unstructured meshes and strict stability for hyperbolic problems.” In: *Applied Numerical Mathematics* 45.4 (2003), pp. 453–473. doi: 10.1016/S0168-9274(02)00239-8.
- [46] P. Öffner. *Error boundedness of Correction Procedure via Reconstruction / Flux Reconstruction*. 2018. arXiv: 1806.01575 [math.NA].
- [47] P. Öffner and H. Ranocha. “Error Boundedness of Discontinuous Galerkin Methods with Variable Coefficients.” In: *Journal of Scientific Computing* 79.3 (June 2019), pp. 1572–1607. doi: 10.1007/s10915-018-00902-1. arXiv: 1806.02018 [math.NA].
- [48] V. Petviashvili. “Equation of an extraordinary soliton (ion acoustic wave packet dispersion in plasma).” In: *Soviet Journal of Plasma Physics* 2 (1976), p. 257.
- [49] C. Rackauckas and Q. Nie. “DifferentialEquations.jl – A Performant and Feature-Rich Ecosystem for Solving Differential Equations in Julia.” In: *Journal of Open Research Software* 5.1 (2017), p. 15. doi: 10.5334/jors.151.
- [50] H. Ranocha. “Generalised Summation-by-Parts Operators and Entropy Stability of Numerical Methods for Hyperbolic Balance Laws.” PhD thesis. TU Braunschweig, Feb. 2018.
- [51] H. Ranocha. “Generalised Summation-by-Parts Operators and Variable Coefficients.” In: *Journal of Computational Physics* 362 (Feb. 2018), pp. 20–48. doi: 10.1016/j.jcp.2018.02.021. arXiv: 1705.10541 [math.NA].
- [52] H. Ranocha. “Mimetic Properties of Difference Operators: Product and Chain Rules as for Functions of Bounded Variation and Entropy Stability of Second Derivatives.” In: *BIT Numerical Mathematics* 59.2 (June 2019), pp. 547–563. doi: 10.1007/s10543-018-0736-7. arXiv: 1805.09126 [math.NA].
- [53] H. Ranocha. “Shallow water equations: Split-form, entropy stable, well-balanced, and positivity preserving numerical methods.” In: *GEM – International Journal on Geomathematics* 8.1 (Apr. 2017), pp. 85–133. doi: 10.1007/s13137-016-0089-9. arXiv: 1609.08029 [math.NA].
- [54] H. Ranocha, L. Dalcin, and M. Parsani. “Fully-Discrete Explicit Locally Entropy-Stable Schemes for the Compressible Euler and Navier-Stokes Equations.” In: *Computers and Mathematics with Applications* 80.5 (July 2020), pp. 1343–1359. doi: 10.1016/j.camwa.2020.06.016. arXiv: 2003.08831 [math.NA].
- [55] H. Ranocha and D. I. Ketcheson. “Relaxation Runge-Kutta Methods for Hamiltonian Problems.” In: *Journal of Scientific Computing* 84.1 (July 2020). doi: 10.1007/s10915-020-01277-y. arXiv: 2001.04826 [math.NA].
- [56] H. Ranocha, L. Lóczi, and D. I. Ketcheson. “General Relaxation Methods for Initial-Value Problems with Application to Multistep Schemes.” In: *Numerische Mathematik* 146 (Oct. 2020), pp. 875–906. doi: 10.1007/s00211-020-01158-4. arXiv: 2003.03012 [math.NA].
- [57] H. Ranocha, M. Quezada de Luna, and D. I. Ketcheson. *Dispersive-wave-error-growth-notebooks. On the Rate of Error Growth in Time for Numerical Solutions of Nonlinear Dispersive Wave Equations*. <https://github.com/ranocha/Dispersive-wave-error-growth-notebooks>. Feb. 2021. doi: 10.5281/zenodo.4540467.
- [58] H. Ranocha, D. Mitsotakis, and D. I. Ketcheson. *A Broad Class of Conservative Numerical Methods for Dispersive Wave Equations*. Accepted in *Communications in Computational Physics*. Nov. 2020. arXiv: 2006.14802 [math.NA].



- [59] H. Ranocha, P. Öffner, and T. Sonar. “Summation-by-parts operators for correction procedure via reconstruction.” In: *Journal of Computational Physics* 311 (Apr. 2016), pp. 299–328. DOI: 10.1016/j.jcp.2016.02.009. arXiv: 1511.02052 [math.NA].
- [60] H. Ranocha, M. Sayyari, L. Dalcin, M. Parsani, and D. I. Ketcheson. “Relaxation Runge-Kutta Methods: Fully-Discrete Explicit Entropy-Stable Schemes for the Compressible Euler and Navier-Stokes Equations.” In: *SIAM Journal on Scientific Computing* 42.2 (Mar. 2020), A612–A638. DOI: 10.1137/19M1263480. arXiv: 1905.09129 [math.NA].
- [61] R. D. Richtmyer and K. W. Morton. *Difference Methods for Boundary-Value Problems*. New York, London, Sydney: John Wiley & Sons, 1967.
- [62] J. M. Sanz-Serna. “An explicit finite-difference scheme with exact conservation properties.” In: *Journal of Computational Physics* 47.2 (1982), pp. 199–210. DOI: 10.1016/0021-9991(82)90074-2.
- [63] J. M. Sanz-Serna and V. Manoranjan. “A method for the integration in time of certain partial differential equations.” In: *Journal of Computational Physics* 52.2 (1983), pp. 273–289. DOI: 10.1016/0021-9991(83)90031-1.
- [64] N. Shima, Y. Kuya, Y. Tamaki, and S. Kawai. “Preventing spurious pressure oscillations in split convective form discretization for compressible flows.” In: *Journal of Computational Physics* (2020), p. 110060. DOI: 10.1016/j.jcp.2020.110060.
- [65] B. Strand. “Summation by Parts for Finite Difference Approximations for  $d/dx$ .” In: *Journal of Computational Physics* 110.1 (1994), pp. 47–67. DOI: 10.1006/jcph.1994.1005.
- [66] M. Svärd and J. Nordström. “Review of summation-by-parts schemes for initial-boundary-value problems.” In: *Journal of Computational Physics* 268 (2014), pp. 17–38. DOI: 10.1016/j.jcp.2014.02.031.
- [67] E. Tadmor. “The numerical viscosity of entropy stable schemes for systems of conservation laws. I.” In: *Mathematics of Computation* 49.179 (1987), pp. 91–103. DOI: 10.1090/S0025-5718-1987-0890255-3.
- [68] C. Tsitouras. “Runge-Kutta pairs of order 5 (4) satisfying only the first column simplifying assumption.” In: *Computers & Mathematics with Applications* 62.2 (2011), pp. 770–775. DOI: 10.1016/j.camwa.2011.06.002.
- [69] G. B. Whitham. “Variational methods and applications to water waves.” In: *Proceedings of the Royal Society of London. Series A. Mathematical and Physical Sciences* 299.1456 (1967), pp. 6–25. DOI: 10.1098/rspa.1967.0119.
- [70] N. Wintermeyer, A. R. Winters, G. J. Gassner, and D. A. Kopriva. “An entropy stable nodal discontinuous Galerkin method for the two dimensional shallow water equations on unstructured curvilinear meshes with discontinuous bathymetry.” In: *Journal of Computational Physics* 340 (2017), pp. 200–242. DOI: 10.1016/j.jcp.2017.03.036.
- [71] A. R. Winters, R. C. Moura, G. Mengaldo, G. J. Gassner, S. Walch, J. Peiro, and S. J. Sherwin. “A comparative study on polynomial dealiasing and split form discontinuous Galerkin schemes for under-resolved turbulence computations.” In: *Journal of Computational Physics* 372 (2018), pp. 1–21. DOI: 10.1016/j.jcp.2018.06.016.